Design, Fabrication, and Thermal Evaluation of a Solar Cooking System Integrated With Tracking Device and Sensible Heat Storage Materials

Clement A. Komolafe[1]* and Clinton E. Okonkwo[2]

[1]Department of Mechanical Engineering, College of Engineering, Landmark University, Omu Aran, Nigeria, [2]Department of Agricultural and Biosystems Engineering, College of Engineering, Landmark University, Omu Aran, Nigeria

Energy need for cooking in both the rural and urban areas all over the world is increasing every day as a result of an increase in population. The consequence of global warming due to the usage of fuels such as fossil fuel, firewood, and other biomass products for cooking necessitates innovative techniques that will improve the standard of living of people. In this study, the design, fabrication, and thermal evaluation of a solar cooking system integrated with an Arduino-based tracking device and sensible heat storage (SHS) materials was investigated. During the water boiling trials with black oil sensible material (BOSHSM), the obtained maximum temperatures for water, cooking box, and sensible heat storage material at 14:00 h when the solar radiation attained its peak value of 881.2 W/m^2 were 64,52, and 54°C, respectively, while at 14:00 h with Black coated granite sensible heat storage material (BCGSHSM) at the solar radiation peak value of 890.4 W/m^2, the maximum temperatures for water, cooking box, and sensible heat storage material were 73.5, 76, and 59°C, respectively. The maximum cooking power and thermal efficiency obtained from the water boiling trials were 48.4 and 56.4 W, and 31.6 and 35.8% respectively. Also, the results from the cooking of edibles revealed that the cooking power values ranged between 42.5 and 58.2, while that of efficiency ranged between 34.5 and 40.3% respectively. The maximum solar radiation during the cooking trial period was 986, 975, 956, and 953 W/m^2. In general, from the results, the developed solar cooking system is a viable alternative to cooking with traditional/open burning of wood or other biomass products that pose a serious environmental and health-related threat to the people living in developing countries.

Keywords: design, cooking, cooking power, thermal efficiency, heat storage materials, modelling, energy

1 INTRODUCTION

Cooking is one of the major domestic activities that require energy for human sustenance. All over the world, energy for cooking is being sourced for using different types of cooking fuels such as fossil fuels, firewood, charcoal, etc. are in use. Due to the increase in the cost of cooking gas, fossil fuel, and also the epileptic nature of power supplies in developing countries, the majority of people in the rural and urban areas still use firewood for cooking (Komolafe and Awogbemi, 2010). Burning of firewood, charcoal, or crop residue, slash and burn agriculture, and deforestation account for 5–20% of all

TABLE 1 | Previously designed solar cooking systems.

References	Design	Results
Hussein et al. (2008)	Experimental investigation of novel indirect solar cooker with indoor PCM thermal storage and cooking unit	The results indicated that the deeveloped cooker could be used to cook different meal at noon and evening time
Kumaresan et al. (2016)	Performance assessment of a solar domestic unit integrated with thermal energy storage system	The maximum temperature reached by the olive oil during the cooking experiment was 152°C within a duration of 15 min
Yadav et al. (2017)	Thermal performance evaluation of solar cooker with latent and sensible heat storage unit for evening cooking	The results revealed that PCM-stone pebbles cases stored 3 to 3.5 times heat compared to PCM-iron gritd and PCM-ron ball cases
Bhave and Thakare (2018)	Development of a solar thermal storage cum cooking device using salt hydrate	The developed cooking device was able to store a charge of heat in about and cook about 140 gm of rice with stored heat in 50 and 30 min Respectively
Saxena and Karakilcik (2017)	A solar box cooker for thermal performance evaluation with low cost thermal storage (sand and grannular carbon)	The thermal efficiency, cooking power and overall heat loss coefficient were 37.1%, 44.81 W, and 3.01 W/m^2°C respectively
Coccia et al. (2018)	A high-temperature solar box cooker with solar-salt-based thermal storage unit	It was found that when the solar radiation was unavailable, the PCM thermal storage improved significantly thermal stabilization of the load
Saxena and Agarwal (2018)	A new hybrid solar cooker with air duct performance characteristics	The thermal efficiency, cooking power and overall heat loss coefficient were 45.11%, 60.20 W, and 6.01 W/m^2 °C respectively. Capable of cooking edibles with 200 W under poor ambient condition
Keith et al. (2019)	A parabolic solar cooker incorporating phase change material	The proposed solar cooker was capable of providing meals for refugee at reasonable cooking times
Omara et al. (2020)	Solar cooking performance using phase change materials	The paper indicated the feasibility of phase change materials for improving the cookeer's perfomance evaluation and thermal parameters
Saxena et al. (2020)	Design and investigation of thermal performance of a box cooker with flexible solar collector tubes	The designed cooker perfomed better than solar box cooker and other designs using thermal energy materials in terms of efficiency, overall heat overall loss coefficient, cooking power, and heat transfer coefficent values of 53.81%, 5.11 W/m^2 °C, 68.81 and 56.78 W/m^2 °C respectively
Khallaf et al. (2020)	Mathematical modelling and experimental validation of thermal performance of a novel design solar cooker	The proposed design used water and glycerin as cooking fluids with maximum efficiencies of 35 and 92%
Hosseinzadeh et al. (2021)	The performance improvement of an indirect solar cooker using multi-walled carbon nano tube-oil nanofluid	From the results, the overall energy efficiency of the cooker with 0.5 w% was 20.08%, while the relative improvement of the overall exergy efficiency of cookers with 0.2 and 0.5 wt% in comparison with cooker wit thermal oil were 37.30 and 65.87% respectively

carbon emissions worldwide (Smith et al., 1993). Energy experts all over the world have recently become more conscious of the adverse effects of global warming as a result of the usage of non-environmental and eco-friendly fuels such as fossil fuel, firewood, charcoal, etc. Harnessing the abundant potentials in the freely given renewable energy source (Sun) which is clean, safe, and readily available for cooking has become a burning issue and most attractive alternative. History made it clear that the idea of using solar energy for cooking started in 1,650 as a result of fuel shortages and rationing arising from the second world war (Wentzel and Pouris, 2007). Using solar cooking would not only eliminate or at least reduce the respiratory illness arising from the exposure to smoke but could also be used to defeat another scourge of the developing world, contaminated water (Tucker, 1999). Solar cookers are classified broadly into two categories, the box, and the concentrating type. The box-type permits solar radiation directly through the glass window for cooking while the concentrating type uses parabolic or spherical, linear fresnel reflectors and a central receiver tower with the cooking pot positioned at the focal point where the Sun rays are focussed (Kumaresan et al., 2016; Noman et al., 2019).

Several studies on various configurations of the box and concentrating types of solar cookers have been reported (Kumar et al., 2008; Akoy and Ahmed, 2015; Hafez et al., 2016; Noman et al., 2019). However, in an attempt to increase the performance of solar cooking systems, researchers have suggested the use of thermal storage materials (sensible, latent heat, and thermochemical). Sensible and latent thermal energy storage has become a critical feature of energy management, with prominence in the effective use and reuse of waste heat and solar energy not only in manufacturing and buildings but also for cooking (Goldstein et al., 2006). The use of thermal energy storage is crucial whenever there is a mismatch between the supply and demand for energy. Based on the cost of the three identified types of thermal storage materials, sensible thermal storage materials is cheaper and readily available for people in rural areas and some urban areas of developing countries like Nigeria. **Table 1** presents the summary of studies on solar cooker with thermal storage materials (Hussein et al., 2008; Saxena et al., 2013a; Saxena et al., 2013b; Kumaresan et al., 2016; Saxena and Karakilcik, 2017; Yadav et al., 2017; Bhave and Thakare, 2018; Coccia et al., 2018; Saxena and Agarwal, 2018; Keith et al., 2019; Khallaf et al., 2020; Omara et al., 2020; Saxena et al., 2020; Hosseinzadeh et al., 2021; Kanyowa et al., 2021). Some authors have reported integration of tracking device (Sun tracker) (Roth et al., 2005; Regin et al., 2008; Skouri et al., 2016; Herez et al., 2018; Babu et al., 2019). (Roth et al., 2005; Regin et al., 2008; Skouri et al., 2016; Herez et al., 2018; Babu et al., 2019). However, heating of the cooking pot/vessel through the parabolic dish and cooking box at the same time has not been reported.

In this study, therefore, design, fabrication, and thermal evaluation of a solar cooking system integrated with a photovoltaic controlled Arduino-based data logging cum

TABLE 2 | Measuring instruments specifications.

S/N	Parameter	Measuring device	Range
1	Temperature	DS18B20 sensor	−55 to +225
2	Humidity	DHT22 sensor	0–100%
3	Wind speed	Digital Thermo-anemometer Lutrom 4201A	0.4–45 m/s
4	Solar radiation	Solar power meter (Pyranometer)	0–2000 W/m2
5	Weighing balance	Digital weighing balance (Model no:D0630/30 Max.)	0.1–30 kg

TABLE 3 | Thermo-physical properties of engine oil (Sharma et al., 2009).

Properties	Value
Density	888 kg/m^3
Specific heat capacity	1.88 kJ/kg/kgK
Thermal conductivity	0.144 W/mK
Thermal diffusivity	8.53×10^{-8} m^2/s/

TABLE 4 | Thermo-physical properties of granite (Bejan and Kraus, 2003).

Properties	Value
Density	2,750 kg/m^3
Specific heat capacity	0.89 kJ/kg/kgK
Thermal conductivity	2.9 W/mK
Thermal diffusivity	0.012 cm^2/s

tracking device and sensible heat storage materials (Black coated granite and used engine oil) for both the rural and urban areas are presented.

2 MATERIALS AND METHODS

2.1 Material Selection

Locally sourced and eco-friendly materials such as aluminum sheet, angle iron, mild steel pipes, plywood, reflective glass, Rockwool, aluminum foil, etc. were selected for the fabrication solar cooking system based on design consideration, preliminary investigation, etc. Also, black coated granite and used black engine oil (black) were used as sensible heat storage materials. Fresh and clean samples of sweet potato and plantain purchased from the neighbouring market were used for the performance evaluation of the cooking system. The measuring instruments and thermophysical properties of SHS are shown in **Tables 2–4** respectively.

2.2 Description of the Parabolic Solar Cooker

The experimental set-up of the fabricated solar cooking system is presented schematically and pictorially as shown in **Figures 1, 2** respectively. It comprises mainly four components namely: the
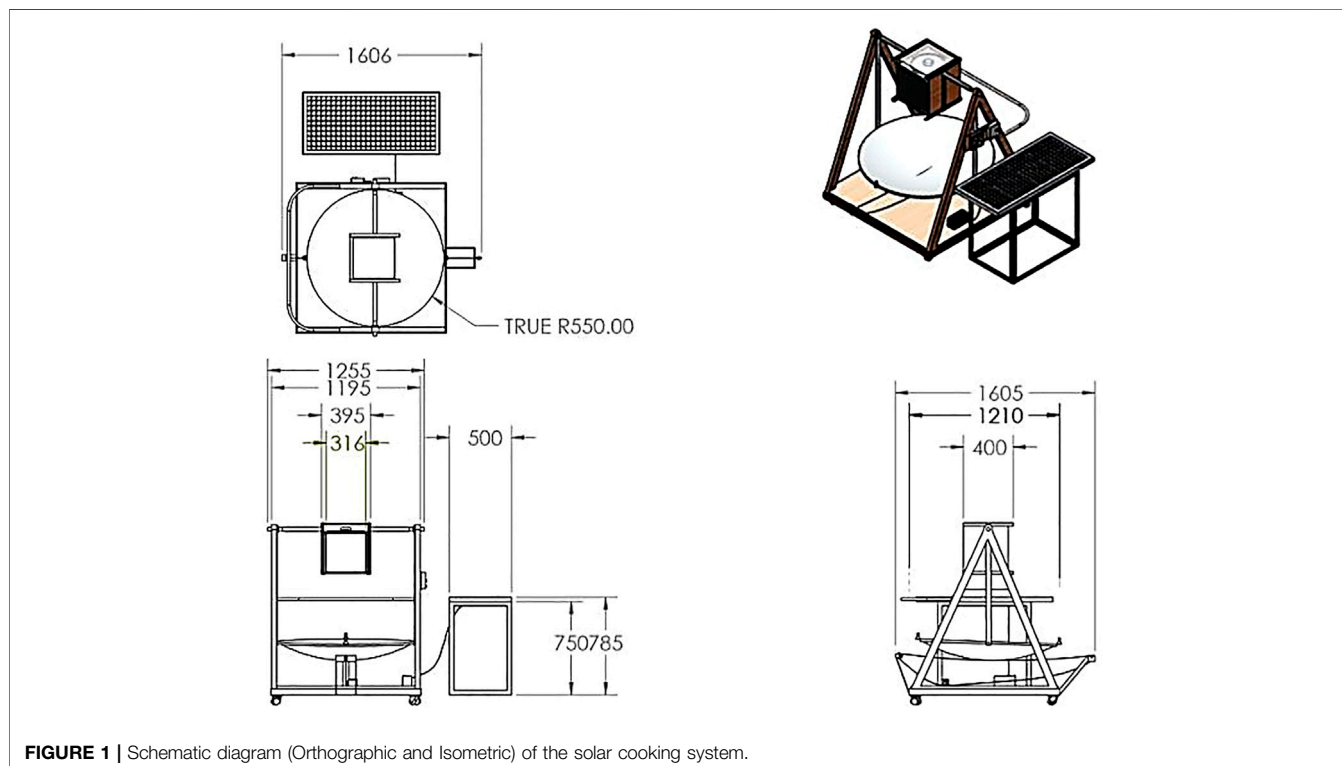

FIGURE 1 | Schematic diagram (Orthographic and Isometric) of the solar cooking system.

1. Cooking box 2. Data Acquisition and solar tracking control unit 3. Parabolic collector/reflector
4. Stepper motor 5. Solar panel connected to Battery

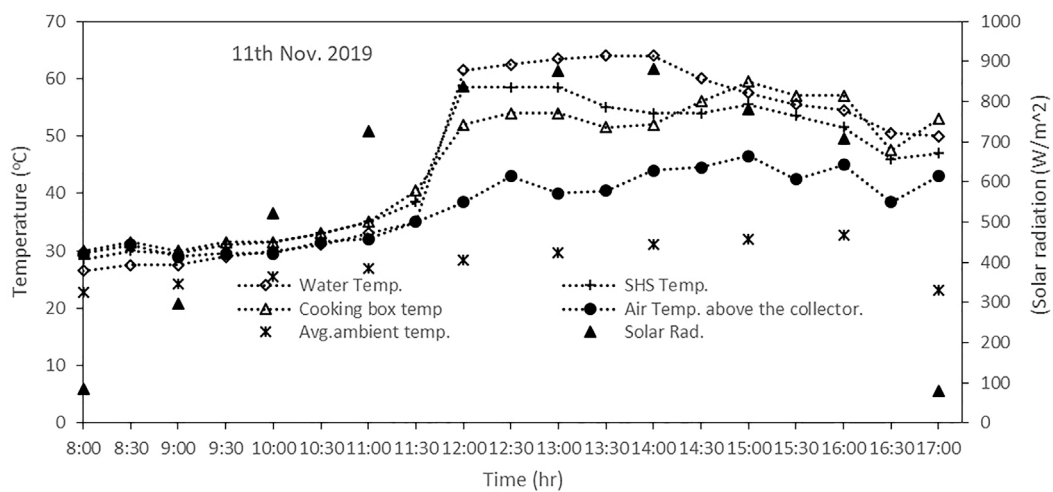**FIGURE 2 |** Pictorial view of the experimental set-up.

FIGURE 3 | The plot of solar radiation and the temperature of the water, cooking box, SHS material, and air against time.

parabolic solar reflector, cooking box, data acquisition and tracking device and supporting frame.

(a) Parabolic reflector: The reflector was fabricated from an aluminum sheet. It is 110 mm in diameter and 150 mm deep. It was cut and glued to the parabolic reflector's surface.

(b) Cooking box: The cooking box has an overall dimension of $1,376 \times 1203 \times 1,203$ mm. It has three of its sides made of wood (lagged with Rockwool for insulation) and the other three reflective glass. The three glasses were located at the top, bottom, and one of the sides of the box to allow the Sun rays into the cooking pot. Inside the cooking box, were a cooking pot made of aluminum sheet and a compartment for heat storage material as shown in **Figure 3**.

(c) Data acquisition and tracking device: The data acquisition and tracking device consists of eight major components namely; micro-controller, Bluetooth module, SD card, real-time clock, temperature sensors (DS18B20), Humidity sensor (DHT22), battery, solar panel, and stepper motor.

2.3 Experimental Procedure

Water boiling and cooking tests were carried out in November 2019 between 8:00 and 17:00 h to evaluate the performance of the tracking device integrated cooking system using black-coated gravel and used engine oil. The experimentation site was Teaching and Research Farm, Landmark University, Omu Aran, Nigeria which is located at latitude 8.8°N, longitude 5.5°E. Prior to the cooking tests, water boiling trials were

conducted in order to ascertain the thermal response of the system with SHS materials. Thereafter, two edibles (Rice and plantain) were used for the cooking tests. The time, date, relative humidity and temperature of water in the pot and other locations within the cooking system data were programmed to be collected by the micro-controller (Atmeg) from the real-time clock chip (DS1307) and stores it in the SD card at intervals of 10 min. The stored temperature solar radiation, data were retrieved from the solar cooker via the Bluetooth connection without any physical contact with the SD card or device. Data for solar radiation, relative humidity, wind speed and ambient temperature were also monitored and recorded for comparison with readings from the installed Campbell Scientific Ltd. made metrological station at Landmark University Teaching and Research Farm which is just a few centimetres away from where the solar cooking system was positioned. The solar tracking device tracks the Sun with the help of two light sensors and a stepper motor. The two LDR (Light dependent renters) were used to monitor the light rays at opposite sides of the parabolic dish. The microcontroller was also configured and programmed to monitor the direction of light rays and to move the parabolic collector with the aid of a stepper motor towards the direction of the sensor with higher light rays. However, when the light ray sensors on both sides sense an equal ray of light, the stepper motor adjusts and position the parabolic reflector at the centre. Specification of measuring device is shown in **Table 1**.

2.4 Theory and Analysis
2.4.1 Parabolic Concentrator
Various components of the solar cooking system were designed using the following parameters (Stine and Diver, 1994; Sup et al., 2015; Hafez et al., 2016; González-Avilés et al., 2018; Babu et al., 2019; Noman et al., 2019; Ahmed et al., 2020).

Parabolic concentrator's aperture area.

The concentrator aperture area, which according to Affandi *et al.* (Affandi et al., 2014) is defined as the area that receives the solar radiation is given by (Hafez et al., 2016; Yahuza et al., 2016)

$$A_{pc} = \frac{\pi D_{pc}^2}{4} \qquad (1)$$

Receiver's aperture area.

The aperture area of the receiver is given by **Eq. 2** (Hafez et al., 2016) as:

$$A_{rc} = \frac{\pi D_{rc}^2}{4} \qquad (2)$$

Area concentration ratio.

The area concentration ratio is defined as the ratio of concentrator aperture area to the receiver aperture area (Affandi et al., 2014)

$$C_r = \frac{A_{pc}}{A_{rc}} \qquad (3)$$

Parabolic dish surface area.

The surface area of the parabolic dish can be determined by **Eq. 4** (El Ouederni et al., 2009)

$$A_s = \frac{8\pi}{3} f^2 \left[\left(1 + \left(D_{ap} \middle/ 4f \right)^2 \right)^{3/2} - 1 \right] \qquad (4)$$

Parabolic dish focal length.

The focal length of the focal point from the parabolic dish concentrator can be expressed as **Eqs 5, 6** (Hafez et al., 2016)

$$f = \frac{D_{pc}}{4 \tan\left(\frac{\Phi_{rim}}{2}\right)} \qquad (5)$$

$$h = \frac{D_{pc}^2}{16 f} \qquad (6)$$

Rim angle.

The rim angle according to Stine (Stine and Diver, 1994), is the angle measured at the focus from the axis to the rim of the solar parabolic truncated. It can be determined using [7]

$$\varphi_{rim} = tan^{-1} \left[\frac{8f/D_r}{16\left(\frac{f}{D_{ap}}\right)^2 - 1} \right] \qquad (7)$$

2.4.2 Design Theory for Solar Radiation
Total solar radiation on tilted surface.

The total incident solar radiation on the tilted surface (I_{Tc}) which is the sum of the three components of beam radiation (I_{bc}), radiation from the sky diffuse (I_{dc}), and ground reflected solar radiation (I_{rc}) can be obtained as (Goswami et al., 2000; Duffie et al., 2020):

$$I_{Tc} = I_{bc} + I_{dc} + I_{rc} \qquad (8)$$

The instantaneous beam radiation on the surface per unit area can be calculated as:

$$I_{bc} = I_{bN} \cos\theta \qquad (9)$$

The angle of incidence (θ) which is the angle between the normal to the surface and a line collinear with the Sun's ray) is related to the solar angle (Goswami et al., 2000):

$$\cos\theta = \cos\alpha \cos(a_s - a_w)sin\beta + \sin\alpha \cos\beta \qquad (10)$$

where α = solar altitude angle, a_s = solar azimuth angle, a_w = panel azimuth angle, β = panel tilt angle.

The surface diffuse radiation (I_{dc}) can be expressed as the product of sky diffuse radiation on the horizontal surface (I_{dh}) and the view factor between the sky and the surface:

$$I_{dc} = I_{dh} \left(1 + cos\beta\right)/2 \qquad (11)$$

The ground reflected solar radiation can be calculated by multiplying the total solar radiation from the total solar incident on the horizontal surface by the ground reflectance (σ) as:

$$I_{rc} = I_h \sigma \qquad (12)$$

2.4.3 Thermal Modelling
The available energy is absorbed by the cooking fluid while the unavailable is lost to the surrounding by convection and

radiation. The energy balance equations for various components of the cooking system namely; the parabolic reflector, Vessel (cooking pot), vessel fluid, energy storage material, cooking box glass cover and the enclosed air cover were written (Mbodji and Hajji, 2017; Yettou et al., 2019; Khallaf et al., 2020; Bhavani et al., 2021). The following assumptions were made:

a. Thermo-physical properties of air, glass, and reflector/absorber remain constant within the cooker temperature range.
b. Proper thermal contact between cooking pot and reflector/absorber surface of the cooker.
c. Negligible heat transfer by reflection between the sidewalls and cooking pot.
d. Exchange of heat as a result of air within the lid covered pot not considered.

Energy balance for the parabolic reflector:

$$\left(mC_{pa}\right)_{ref}\frac{dT_{ref}}{dt} = \alpha_{ref}A_{ref}IN + Q_{r, ref \to pot} - Q_{c,ref \to a} - Q_{r,ref-s} \tag{13}$$

Energy balance for the vessel (cooking pot):

$$\left(mC_{pa}\right)_{pot}\frac{dT_{pot}}{dt} = \alpha_{pot}A_{spot}AR - Q_{c,pot \to wat} - Q_{c,pot \to a} \\ - Q_{r, ref \to pot} - Q_{r,pot \to s} \tag{14}$$

Energy balance for fluid in the vessel:

$$\left(mC_{pa}\right)_{wat}\frac{dT_{wat}}{dt} = Q_{c,pot \to wat} \tag{15}$$

Energy balance for the storage material:

$$\left(mC_{pa}\right)_{st}\frac{dT_{st}}{dt} = Q_{r,ref \to st} \tag{16}$$

Energy balance for the cooking box glass cover

$$\left(mC_{pa}\right)_{gls}\frac{dT_{gls}}{dt} = \tau_{gls}\alpha_{gls}A_{gls}IS + Q_{c,i \to gls} + Q_{r,v,\to gls} - Q_{r,p \to gls} \\ - Q_{c,gls \to a} - Q_{r,gls \to s} - Q_{r,p \to s} \tag{17}$$

Energy balance for the air inside the cooking box

$$\left(mC_{pa}\right)_{i}\frac{dT_{i}}{dt} = Q_{c,p \to i} + Q_{c,v,\to i} - Q_{c,i \to gls} \tag{18}$$

where

$$Q_{c,i \to gls} = h_{c,i-gls}A_{gls}\left(T_{i} - T_{gls}\right) \tag{19}$$

$$Q_{c,gls \to a} = h_{c,gls-a}A_{gls}\left(T_{gls} - T_{a}\right) \tag{20}$$

$$Q_{c,p \to i} = h_{c,p-i}\left(A_{pot} - nA_{vb}\right)\left(T_{pot} - T_{i}\right) \tag{21}$$

$$Q_{c,v \to i} = h_{c,v-i}nA_{v}\left(T_{v} - T_{i}\right) \tag{22}$$

$$Q_{r,gls \to s} = h_{r,gls-s}A_{gls}\left(T_{gls} - T_{s}\right) \tag{23}$$

$$Q_{r,p \to gls} = h_{r,pot-gls}\left(A_{p} - nA_{vb}\right)\left(T_{pot} - T_{gls}\right) \tag{24}$$

$$Q_{r,v \to gls} = h_{r,v-gls}nA_{vb}\left(T_{v} - T_{gls}\right) \tag{25}$$

$$Q_{c,ref \to a} = h_{c,ref-a}A_{ref}\left(T_{ref} - T_{a}\right) \tag{26}$$

$$Q_{c,pot \to a} = h_{c,pot-a}A_{pot}\left(T_{pot} - T_{a}\right) \tag{27}$$

$$Q_{c,pot \to wat} = h_{c,pot-wat}A_{pf}\left(T_{pot} - T_{wat}\right) \tag{28}$$

$$Q_{r, ref \to pot} = h_{r,pot-ref}A_{ref}\left(T_{pot} - T_{ref}\right) \tag{29}$$

$$Q_{r,pot \to s} = h_{r,pot-s}A_{pot}\left(T_{pot} - T_{s}\right) \tag{30}$$

$$Q_{r,ref-s} = h_{r,ref-s}A_{ref}\left(T_{ref} - T_{s}\right) \tag{31}$$

$$Q_{r,ref \to st} = h_{r,ref-s}A_{ref}\left(T_{ref} - T_{s}\right) \tag{32}$$

Substituting the heat transfer flux, the energy balance model **Eqs 13–18** can be written as follows:

- For glass cover

$$\left(mC_{pa}\right)_{gls}\frac{dT_{gls}}{dt} = \tau_{gls}\alpha_{gls}A_{gls}IS + h_{c,i-gls}A_{gls}\left(T_{i} - T_{gls}\right) \\ + h_{r,v-gls}nA_{vb}\left(T_{v} - T_{gls}\right) \\ + h_{r,p-gls}\left(A_{p} - nA_{vb}\right)\left(T_{p} - T_{gls}\right) \\ - h_{c,g-a}A_{gls}\left(T_{gls} - T_{a}\right) - h_{r,gls-s}A_{g}\left(T_{gls} - T_{s}\right) \tag{33}$$

- For the air inside the cooking box

$$\left(mC_{pa}\right)_{i}\frac{dT_{i}}{dt} = h_{c,p-i}\left(A_{pot} - nA_{vb}\right)\left(T_{pot} - T_{i}\right) + h_{c,v-i}nA_{v}\left(T_{v} - T_{i}\right) \\ - h_{c,i-gls}A_{gls}\left(T_{i} - T_{gls}\right) \tag{34}$$

- For Parabolic reflector:

$$\left(mC_{pa}\right)_{ref}\frac{dT_{ref}}{dt} = \alpha_{ref}A_{ref}IN + h_{r,pot-ref}A_{ref}\left(T_{pot} - T_{a}\right) \\ -h_{c,ref-a}A_{ref}\left(T_{ref} - T_{a}\right) - h_{r,ref-s}A_{ref}\left(T_{ref} - T_{s}\right) \tag{35}$$

- For the vessel (cooking pot):

$$\left(mC_{pa}\right)_{pot}\frac{dT_{pot}}{dt} = C_{R}\alpha_{pot}A_{spot}IN - h_{c,pot-wat}A_{pf}\left(T_{pot} - T_{wat}\right) \\ - h_{c,pot-a}A_{pot}\left(T_{pot} - T_{a}\right) - h_{r,pot-ref}A_{ref}\left(T_{pot} \\ - T_{ref}\right) - h_{r,pot-s}A_{pot}\left(T_{pot} - T_{s}\right) \tag{36}$$

- For the vessel fluid:

$$\left(mC_{pa}\right)_{wat}\frac{dT_{wat}}{dt} = h_{c,pot-wat}A_{pf}\left(T_{pot} - T_{wat}\right) \tag{37}$$

- For the storage material

$$\left(mC_{pa}\right)_{st}\frac{dT_{st}}{dt} = h_{r,ref-s}A_{ref}\left(T_{ref} - T_{s}\right) \tag{38}$$

TABLE 5 | The uncertainty of some measure parameters during the experiments.

S/N	Measured parameters	Uncertainty
1	Solar radiation	$\pm 3.42\ W/m^2$
2	Ambient temperature	$\pm 0.48\ °C$
3	Wind velocity	$\pm 0.17\ °C$
4	Thermal efficiency	$\pm 0.89\%$
5	Heat transfer	$\pm 5.1\ W/m^2°C$
6	overall heat loss	$\pm 2.2\ W/m^2°C$ C
7	Plate temperature	$\pm 5.2\ °C$

The coefficient of heat transfer for cooker can be expressed as (Duffie et al., 2020):

$$h = \frac{Q_u}{A_{ap}\left(T_p - T_f\right)} = \frac{\tau I_{av} A_{ap}}{A_{ap}\left(T_p - T_f\right)} \tag{39}$$

Assume the side losses are negligible, the overall heat loss can be obtained as (Channiwala and Doshi, 1989):

$$U_L = \left[\frac{2.8}{\frac{1}{\epsilon_p}\left(\frac{1}{N_c^{0.025}+\epsilon_c}-1\right)} + 0.825\,(x_m)^{0.21} + aV_{win}^{b} - 0.5\left(N_c^{0.025}-1\right)\right]\left(T_{pm}-T_{amb}\right)^{0.2} + \frac{k_i}{+t_i} \tag{40}$$

2.4.4 Standard Cooking Power

The amount of heat that enters the container of the solar cooking system to raise the temperature of a given quantity of water in a certain time interval is known as standard cooking power (P_{sc}). It can be obtained as (Akoy and Ahmed, 2015; González-Avilés et al., 2018):

$$P_{sc} = mC_p \frac{T_f - T_i}{T} \tag{41}$$

where m is the mass of water (kg); C_p is the specific heat of water (4.182 kJ/kg °C); T_f is the final water temperature

(°C); T_w is the initial water temperature (°C); T is the time (s).

2.4.5 Thermal Efficiency

Thermal efficiency is obtained as (Komolafe and Waheed, 2018; Komolafe et al., 2019; Komolafe et al., 2021):

$$\eta = \frac{\dot{m}C_p\left(T_{c\ out} - T_{a\ in}\right)}{I_c A_c} \tag{42}$$

2.5 Uncertainty Analysis

Implementation of the uncertainty analysis is necessary in order to investigate the reliability of the results. The total uncertainty for a measured parameter (P) can be calculated using the following equation (Zamani et al., 2015; Hosseinzadeh et al., 2020): Some measured parameters are shown in **Table 5**.

$$\delta P_{TOT} = \sqrt{\left(\delta p_{equ}\right)^2 + \left(\delta p_{rep}\right)^2} \tag{43}$$

where $\left(\delta p_{equ}\right)^2 \ and \geq \left(\delta p_{rep}\right)^2$ represent the equipment and repetition uncertainties respectively.

The uncertainty function $C = C(p_1,\ p_2\ldots\ldots\ldots p_n)$ which is a function of independent linear parameters can be expressed as (Hosseinzadeh et al., 2021):

$$\delta C = \sqrt{\left(\frac{\delta C}{\delta p_1}\delta p_1\right)^2 + \left(\frac{\delta C}{\delta p_2}\delta p_2\right)^2 + \left(\frac{\delta C}{\delta p_n}\delta p_n\right)^2} \tag{44}$$

3 RESULTS AND DISCUSSION

Figure 3 shows the plot of solar radiation and the temperature of the water, cooking box, sensible heat storage material, and air against time with used engine oil as sensible heat storage material.
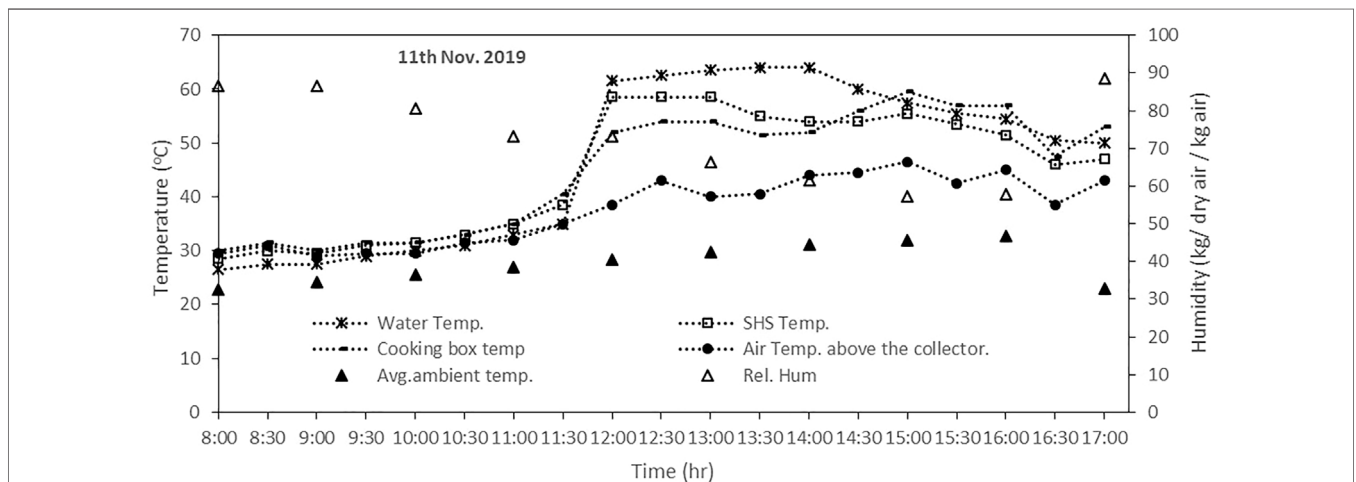

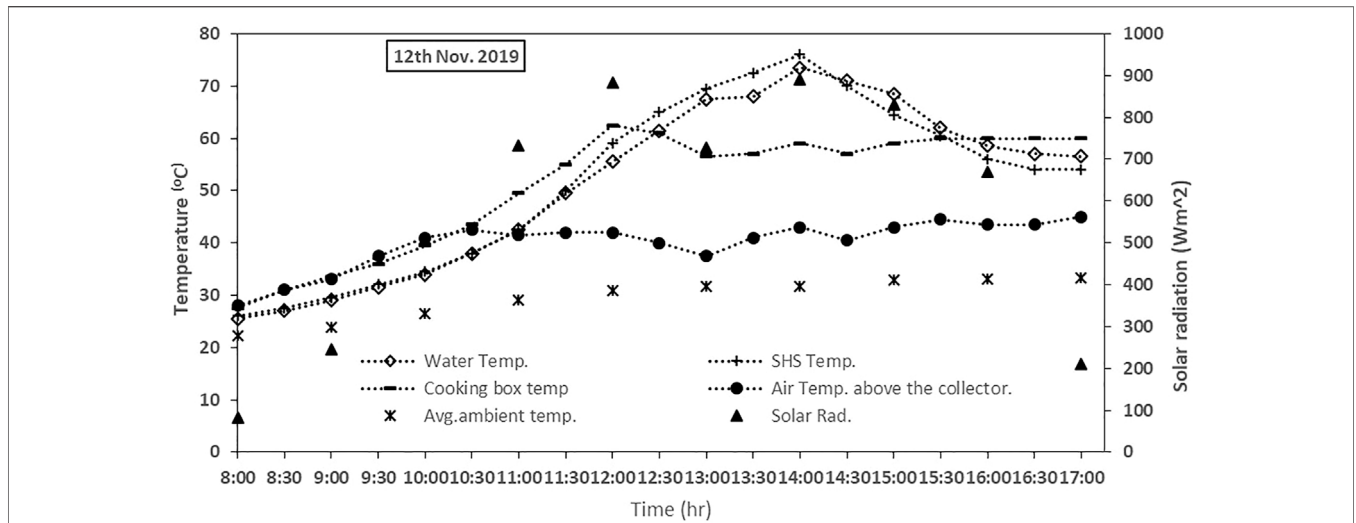**FIGURE 4 |** The plot of humidity and the temperature of the water, cooking box, SHS material, and air against time.

FIGURE 5 | The plot of solar radiation and the temperature of the water, cooking box, SHS material, and air against time.
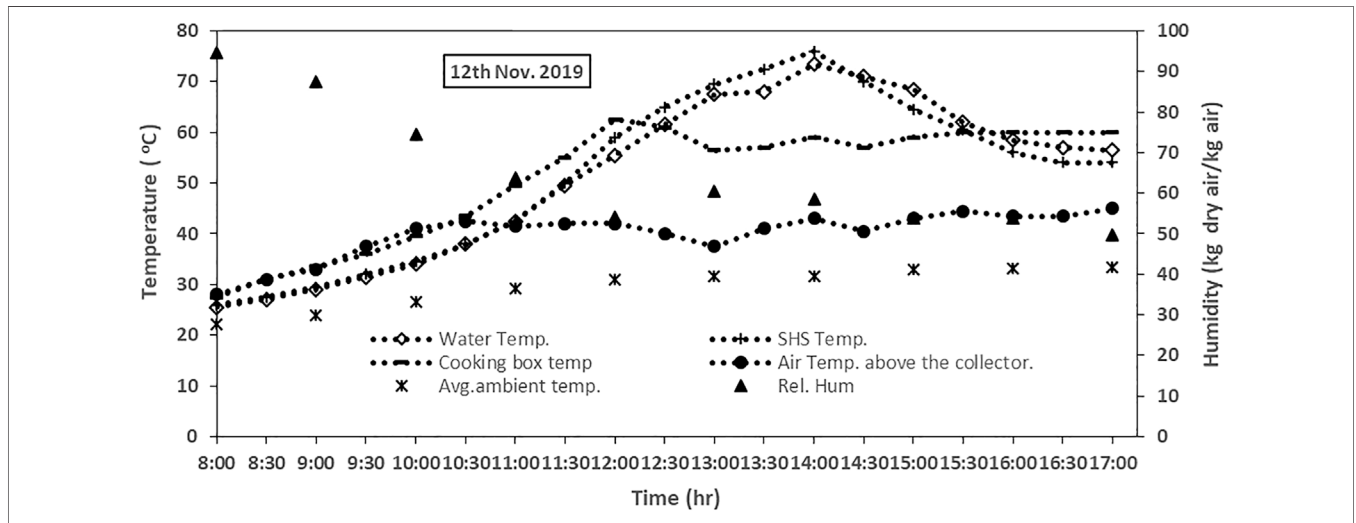

FIGURE 6 | The plot of humidity and the temperature of the water, cooking box, SHS material, and air against time.

It is evident from the figure that the temperature of the water and that of other locations within the cooking system were almost the same in the early hour of the experiment and began to vary from 11:00 h. The observed temperature profile follows the same pattern with the solar radiation. Thus, an increase in solar radiation resulted in to increase in temperature. The obtained maximum temperatures for water, cooking box, and sensible heat storage material at 14:00 h when the solar radiation attained its peak value of 881.2 W/m^2 were 64,52, and 54°C, respectively. The figure further revealed that at 17:00 h when the lowest solar radiation value of 80 W/m^2 was attained, the temperatures of water and the cooking box were 50 and 53°C, respectively. This could be attributed to the incorporation of insulating and heat storage materials into the cooking box.

The variation of relative humidity and the temperature of the water, cooking box, sensible heat storage material, and air against time with used engine oil (black) as heat storage material is shown in **Figure 4**. It can be seen that the relative humidity decreased with time as the temperatures increased. The relative humidity minimum and maximum values of 57.2 and 88.6% were attained at 15:00 and 17:00 h respectively. When compared with **Figure 3**, solar radiation and temperatures decreased as the relative humidity increased and vice versa.

Figure 5 depicts the variation of solar radiation and the temperature of the water, cooking box, sensible heat storage material, and air with time. From the graph, it is evident that the temperature profile follows the same pattern with the solar
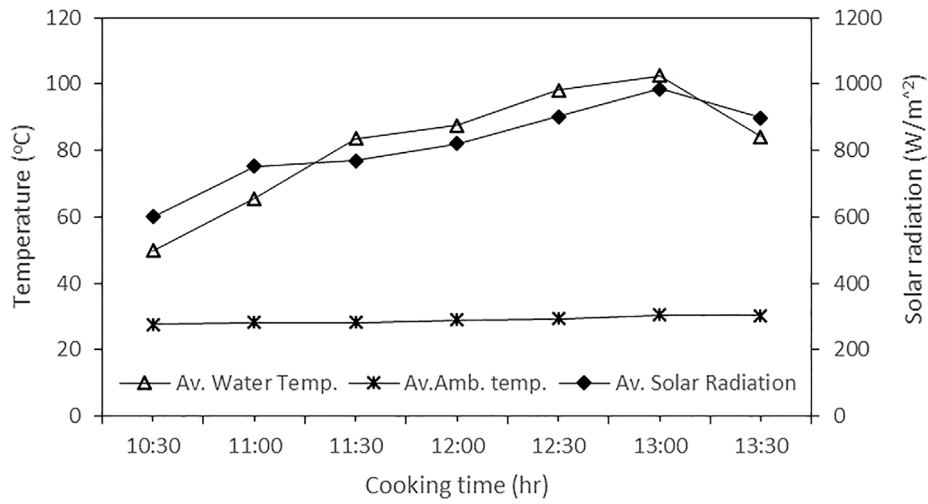
FIGURE 7 | The graph of temperature and solar radiation versus cooking duration of rice using granite as SHS.
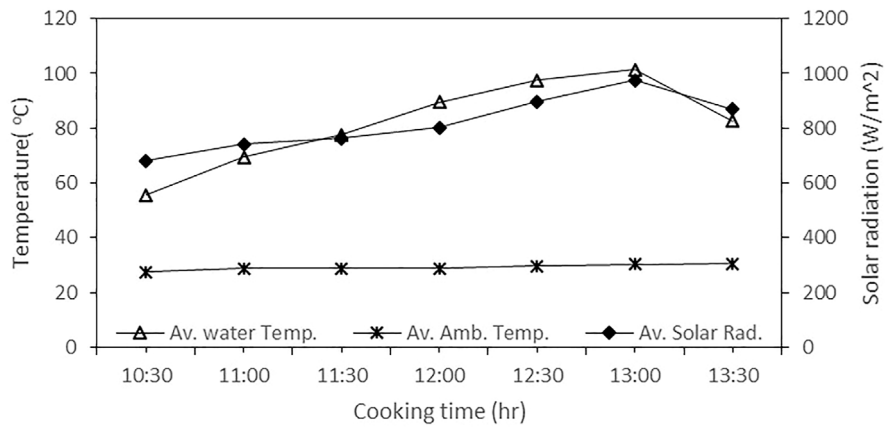

FIGURE 8 | The graph of temperature and solar radiation versus cooking duration of rice using engine oil as SHS material.
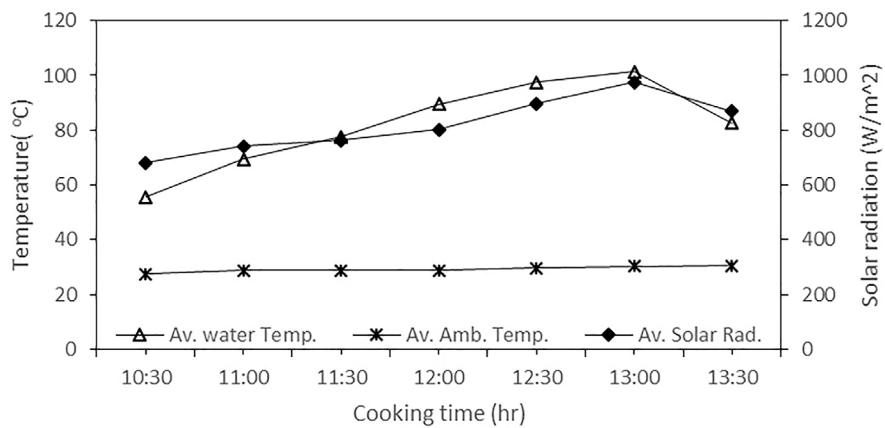

FIGURE 9 | The graph of temperature and solar radiation versus cooking duration Plantain using engine oil as SHS material.
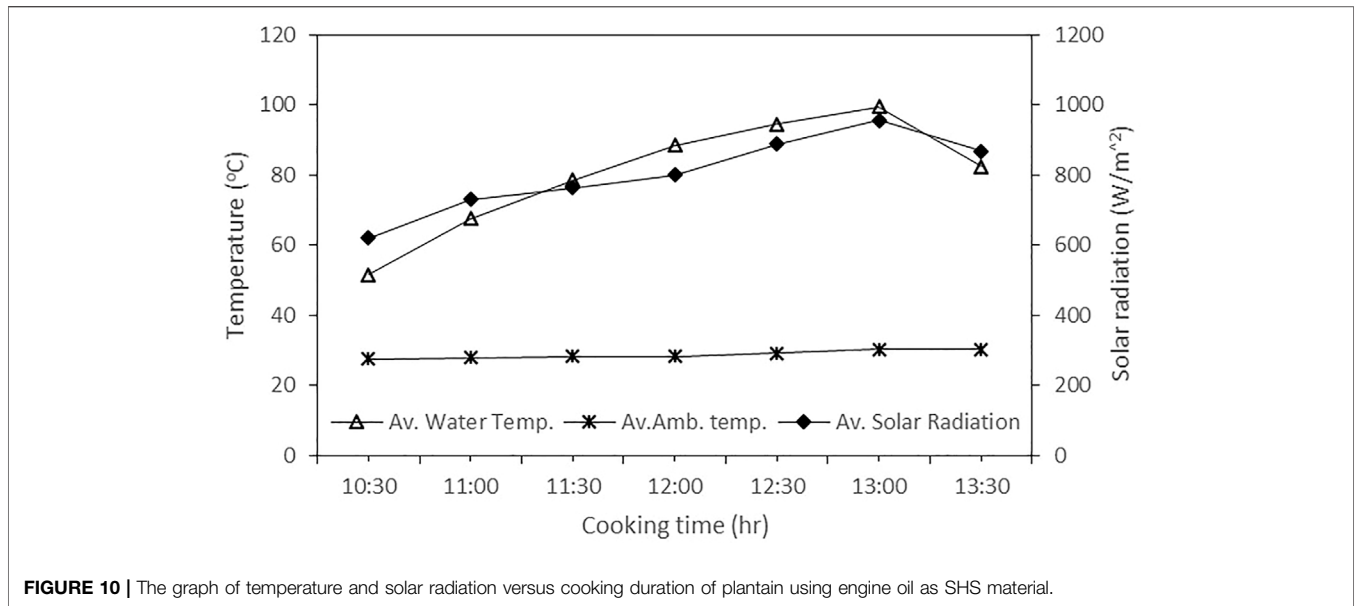
FIGURE 10 | The graph of temperature and solar radiation versus cooking duration of plantain using engine oil as SHS material.

TABLE 6 | Cooking duration for two edibles using SHS materials.

SHS material	Edible material	Mass (kg)	Amb. Temp. (°C)	Time (Min.)	Efficiency (%)	Remark
Granite	Rice	0.8	30.3	144	40.3	Boiled
Engine oil	Rice	0.8	30.4	147	38	Boiled
Granite	Plantain	0.95	30.3	150	36	Boiled
Engine oil	Plantain	0.95	31.5	151	34.5	Boiled

radiation in a similar manner to **Figure 3**. However, the maximum temperatures for water, cooking box, and sensible heat storage material at 14:00 h when the solar radiation attained its peak value of 890.4 W/m^2 were 73.5, 76, and 59°C, respectively. The difference in these temperature values and those reported in **Figure 3** could be attributed to the irregular intensity of solar radiation or the thermal conductivity of the sensible heat storage materials used. Similar reports have been presented by (Komolafe and Waheed, 2018).

Figure 6 presents the plot of humidity and the temperature of the water, cooking box, sensible heat storage material, and air against time using black coated gravel as heat storage material. It can be seen that the relative humidity decreased with time as the temperatures increased. The relative humidity minimum and maximum values of 49.8 and 94.6% were attained at 17:00 and 8:00 h respectively. When compared with **Figure 5**, solar radiation and temperatures decreased as the relative humidity increased and vice versa.

Figure 7 represents the plots of temperature and solar radiation versus cooking duration of rice using black coated granite as SHS material. With water as cooking fluid, 0.8 kg of rice was boiled between 18 and 20th of November 2019. Each experiment was conducted between 10:30 and 13:30 h. From the graph, the average minimum and maximum temperature of water and ambient which occurred at 10: 30 and 13:00 h were 49.7 and

102°C respectively. The average solar radiation at these periods were 600 and 986 W/m^2 respectively.

Figure 8 shows the plots of temperature and solar radiation versus cooking duration of rice using as granite as SHS material. With water as cooking fluid, 0.8 kg of rice was boiled between 21st–23rd of November 2019. Each experiment commenced at 10:30 h and terminated at 13:30 h. It was observed that the average minimum and maximum temperature of water and ambient which occurred at 10: 30 and 13:00 h were 55.5 and 101.5°C respectively, while the average solar radiation at these periods were 680 and 975 W/m^2 respectively.

Figure 9 reveals the plots of temperature and solar radiation versus cooking duration of rice using black engine oil as SHS material. With water as cooking fluid, 0.95 kg of plantain was boiled between 24th–26th of November 2019. Each experiment was conducted between 10:30 and 13:30 h. It was observed that the average minimum and maximum temperature of water and ambient which occurred at 10:30 and 13:00 h were 54 and 100.8°C respectively, while the average solar radiation at these periods were 635 and 956 W/m^2 respectively.

Figure 10 depicts the plots of temperature and solar radiation versus cooking duration of rice using black engine oil as SHS material. With water as cooking fluid, 0.95 kg of plantain was boiled between 27th–30th of November 2019. Each experiment was conducted between 10:30 and 13:30 h. It was observed that the average minimum and maximum temperature of water and ambient which occurred at 10:30 and 13:00 h were 51.5 and 99.5°C respectively, while the average solar radiation at these periods were 635 and 953 W/m^2 respectively. Generally from the graphs, it can be seen that the increase in solar radiation resulted to increase in temperature.

3.1 Cooking Duration
The cooking time, heat capacity, and efficiency obtained from cooking trials are shown in **Table 6**.

3.2 Cooking Power and Thermal Efficiency

The maximum cooking power and thermal efficiency for the water boiling tests under solar cooking system integrated with both black engine oil and black coated gravel were 48.4 and 56.4 W, and 31.6 and 35.8% respectively. However, for the edibles cooking, the cooking power values ranged between 42.5 and 58.2, while that of efficiency ranged between 34.5 and 40.3% respectively.

4 CONCLUSION

In the current study, the design, fabrication, and thermal evaluation of a solar cooking system integrated with tracking device and sensible heat storage materials (granite and engine oil) has been presented. The objective was to address majorly health challenge that is predominant among the people living in the rural area who in most cases use firewood and other biomass product for cooking. Locally sourced materials were used to fabricate the cooker. Thereafter, water boiling and cooking trials were adopted to evaluate the performance of the cooking system. From the results, the following major conclusions were drawn:

1. The obtained maximum solar radiation and water temperature during the water boiling tests with black engine oil as sensible heat storage material at 14:00 h were 881.2 W/m^2 and 64 respectively, while with black coated gravel at this period were 890.4 W/m^2 and 73.5°C.

2. The average cooking duration of rice and plantain with cooking system ranged between 144 and 151 min using black coated granite and black engine oil SHS materials respectively.

3. The maximum cooking power and thermal efficiency obtained from the cooking trials of rice and plantain were 58.2 W and 40.3% respectively.

4. The developed cooker is expected to perform better when the solar intensity is higher

5. Adoption of the developed solar cooking system will reduce environmental pollution that occur when firewood, fossil fuel etc. are used.

6. With minor design modifications, there will be an improvement on the performance of the developed cooking system.

DATA AVAILABILITY STATEMENT

The original contributions presented in the study are included in the article/Supplementary Material, further inquiries can be directed to the corresponding author.

AUTHOR CONTRIBUTIONS

CK: Conceived and design the experiment, performed the experiment, analysed and interpreted the data, wrote the paper. CO: Performed the experiment, wrote the paper.

REFERENCES

Affandi, R., Gan, C. K., Ruddin, M., and ghani, A. (2014). Development of Design Parameters for the Concentrator of Parabolic Dish (Pd) Based Concentrating Solar Power (Csp) under malaysia Environment. *J. Appl. Sci. Agric.* 9, 42–48.

Ahmed, S. M. M., Al-Amin, M. R., Ahammed, S., Ahmed, F., Saleque, A. M., and Abdur Rahman, M. (2020). Design, Construction and Testing of Parabolic Solar Cooker for Rural Households and Refugee Camp. *Solar Energy* 205, 230–240. doi:10.1016/j.solener.2020.05.007

Akoy, E. O., and Ahmed, A. I. (2015). Design, Construction and Performance Evaluation of Solar Cookers. *J. Agric. Sci. Eng.* 1, 75–82.

Babu, M., Raj, S. S., and Valan Arasu, A. (2019). Experimental Analysis on Linear Fresnel Reflector Solar Concentrating Hot Water System with Varying Width Reflectors. *Case Stud. Therm. Eng.* 14, 100444. doi:10.1016/j.csite.2019.100444

Bejan, A., and Kraus, A. D. (2003). *Heat Transfer Handbook*. John Wiley & Sons.

Bhavani, S., Shanmugan, S., Chithambaram, V., Essa, F. A. E., Kabeel, A.-E., and Selvaraju, P. (2021). Simulation Study on thermal Performance of a Solar Box Cooker Using Nanocomposite for Natural Food Invention. *Environ. Sci. Pollut. Res.* 1, 1–19. doi:10.1007/s11356-021-14194-w

Bhave, A. G., and Thakare, K. A. (2018). Development of a Solar thermal Storage Cum Cooking Device Using Salt Hydrate. *Solar Energy* 171, 784–789. doi:10.1016/j.solener.2018.07.018

Channiwala, S. A., and Doshi, N. I. (1989). Heat Loss Coefficients for Box-type Solar Cookers. *Solar Energy* 42, 495–501. doi:10.1016/0038-092x(89)90050-9

Coccia, G., Di Nicola, G., Tomassetti, S., Pierantozzi, M., Chieruzzi, M., and Torre, L. (2018). Experimental Validation of a High-Temperature Solar Box Cooker with a Solar-Salt-Based Thermal Storage Unit. *Solar Energy* 170, 1016–1025. doi:10.1016/j.solener.2018.06.021

Duffie, J. A., Beckman, W. A., and Blair, N. (2020). *Solar Engineering of thermal Processes, Photovoltaics and Wind*. John Wiley & Sons.

El Ouederni, A., Salah, M. B., Askri, F., Nasrallah, M. B., and Aloui, F. (2009). Experimental Study of a Parabolic Solar Concentrator. *Revue des Energies Renouvelables* 12, 395–404.

Goldstein, R. J., Ibele, W. E., Patankar, S. V., Simon, T. W., Kuehn, T. H., Strykowski, P. J., et al. (2006). Heat Transfer-A Review of 2003 Literature. *Int. J. Heat Mass Transfer* 49, 451–534. doi:10.1016/j.ijheatmasstransfer.2005.11.001

González-Avilés, M., Urrieta, O. R., Ruiz, I., and Cerutti, O. M. (2018). Design, Manufacturing, thermal Characterization of a Solar Cooker with Compound Parabolic Concentrator and Assessment of an Integrated Stove Use Monitoring Mechanism. *Energ. Sustainable Development* 45, 135–141.

Goswami, D. Y., Kreith, F., and Kreider, J. F. (2000). *Principles of Solar Engineering*. Phildelphia, PA: CRC Press.

Hafez, A. Z., Soliman, A., El-Metwally, K. A., and Ismail, I. M. (2016). Solar Parabolic Dish Stirling Engine System Design, Simulation, and thermal Analysis. *Energ. Convers. Manag.* 126, 60–75. doi:10.1016/j.enconman.2016.07.067

Herez, A., Ramadan, M., and Khaled, M. (2018). Review on Solar Cooker Systems: Economic and Environmental Study for Different Lebanese Scenarios. *Renew. Sustainable Energ. Rev.* 81, 421–432. doi:10.1016/j.rser.2017.08.021

Hosseinzadeh, M., Faezian, A., Mirzababaee, S. M., and Zamani, H. (2020). Parametric Analysis and Optimization of a Portable Evacuated Tube Solar Cooker. *Energy* 194, 116816. doi:10.1016/j.energy.2019.116816

Hosseinzadeh, M., Sadeghirad, R., Zamani, H., Kianifar, A., and Mirzababaee, S. M. (2021). The Performance Improvement of an Indirect Solar Cooker Using Multi-Walled Carbon Nanotube-Oil Nanofluid: An Experimental Study with Thermodynamic Analysis. *Renew. Energ.* 165, 14–24. doi:10.1016/j.renene.2020.10.078

Hussein, H. M. S., El-Ghetany, H. H., and Nada, S. A. (2008). Experimental Investigation of Novel Indirect Solar Cooker with Indoor PCM thermal Storage and Cooking Unit. *Energ. Convers. Manag.* 49, 2237–2246. doi:10.1016/j.enconman.2008.01.026

Kanyowa, T., Victor Nyakujara, G., Ndala, E., and Das, S. (2021). Performance Analysis of Scheffler Dish Type Solar thermal Cooking System Cooking 6000 Meals Per Day. *Solar Energy* 218, 563–570. doi:10.1016/j.solener.2021.03.019

Keith, A., Brown, N. J., and Zhou, J. L. (2019). The Feasibility of a Collapsible Parabolic Solar Cooker Incorporating Phase Change Materials. *Renew. Energ. Focus* 30, 58–70. doi:10.1016/j.ref.2019.03.005

Khallaf, A. M., Tawfik, M. A., El-Sebaii, A. A., and Sagade, A. A. (2020). Mathematical Modeling and Experimental Validation of the thermal Performance of a Novel Design Solar Cooker. *Solar Energy* 207, 40–50. doi:10.1016/j.solener.2020.06.069

Komolafe, C. A., Oluwaleye, I. O., Awogbemi, O., and Osueke, C. O. (2019). Experimental Investigation and thermal Analysis of Solar Air Heater Having Rectangular Rib Roughness on the Absorber Plate. *Case Stud. Therm. Eng.* 14, 100442. doi:10.1016/j.csite.2019.100442

Komolafe, C. A., and Waheed, M. A. (2018). Design and Fabrication of a Forced Convection Solar Dryer Integrated with Heat Storage Materials. *ACSM* 1, 23–39. doi:10.3166/acsm.42.22-39

Komolafe, C. A., Waheed, M. A., Kuye, S. I., Adewumi, B. A., and Daniel Adejumo, A. O. (2021). Thermodynamic Analysis of Forced Convective Solar Drying of cocoa with Black Coated Sensible thermal Storage Material. *Case Stud. Therm. Eng.* 26, 101140. doi:10.1016/j.csite.2021.101140

Komolafe, C., and Awogbemi, O. (2010). Fabrication and Performance Evaluation of an Improved Charcoal Cooking Stove. *Pac. J. Sci. Technology* 11, 51–58.

Kumar, N., Agravat, S., Chavda, T., and Mistry, H. N. (2008). Design and Development of Efficient Multipurpose Domestic Solar Cookers/dryers. *Renew. Energ.* 33, 2207–2211. doi:10.1016/j.renene.2008.01.010

Kumaresan, G., Vigneswaran, V. S., Esakkimuthu, S., and Velraj, R. (2016). Performance Assessment of a Solar Domestic Cooking Unit Integrated with thermal Energy Storage System. *J. Energ. Storage* 6, 70–79. doi:10.1016/j.est.2016.03.002

Mbodji, N., and Hajji, A. (2017). Modeling, Testing, and Parametric Analysis of a Parabolic Solar Cooking System with Heat Storage for Indoor Cooking. *Energ. Sustainability Soc.* 7, 1–16. doi:10.1186/s13705-017-0134-z

Noman, M., Wasim, A., Ali, M., Jahanzaib, M., Hussain, S., Ali, H. M. K., et al. (2019). An Investigation of a Solar Cooker with Parabolic Trough Concentrator. *Case Stud. Therm. Eng.* 14, 100436. doi:10.1016/j.csite.2019.100436

Omara, A. A. M., Abuelnuor, A. A. A., Mohammed, H. A., Habibi, D., and Younis, O. (2020). Improving Solar Cooker Performance Using Phase Change Materials: A Comprehensive Review. *Solar Energy* 207, 539–563. doi:10.1016/j.solener.2020.07.015

Regin, A. F., Solanki, S. C., and Saini, J. S. (2008). Heat Transfer Characteristics of thermal Energy Storage System Using PCM Capsules: a Review. *Renew. Sustainable Energ. Rev.* 12, 2438–2458. doi:10.1016/j.rser.2007.06.009

Roth, P., Georgiev, A., and Boudinov, H. (2005). Cheap Two axis Sun Following Device. *Energ. Convers. Manag.* 46, 1179–1192. doi:10.1016/j.enconman.2004.06.015

Saxena, A., and Agarwal, N. (2018). Performance Characteristics of a New Hybrid Solar Cooker with Air Duct. *Solar Energy* 159, 628–637. doi:10.1016/j.solener.2017.11.043

Saxena, A., Cuce, E., Tiwari, G. N., and Kumar, A. (2020). Design and thermal Performance Investigation of a Box Cooker with Flexible Solar Collector Tubes: An Experimental Research. *Energy* 206, 118144. doi:10.1016/j.energy.2020.118144

Saxena, A., and Karakilcik, M. (2017). Performance Evaluation of a Solar Cooker with Low Cost Heat Storage Material. *Ijsge* 6, 57–63. doi:10.11648/j.ijrse.20170604.12

Saxena, A., Lath, S., and Tirth, V. (2013a). Solar Cooking by Using PCM as a thermal Heat Storage. *MIT Int. J. Mech. Eng.* 3, 91–95.

Saxena, A., Lath, S., and Tirth, V. (2013b). Solar Cooking by Using PCM as a thermal Heat Storage. *MIT Int. J. Mech. Eng.* 3, 91–95.

Sharma, A., Tyagi, V. V., Chen, C. R., and Buddhi, D. (2009). Review on thermal Energy Storage with Phase Change Materials and Applications. *Renew. Sustainable Energ. Rev.* 13, 318–345. doi:10.1016/j.rser.2007.10.005

Skouri, S., Ben Haj Ali, A., Bouadila, S., Ben Salah, M., and Ben Nasrallah, S. (2016). Design and Construction of Sun Tracking Systems for Solar Parabolic Concentrator Displacement. *Renew. Sustainable Energ. Rev.* 60, 1419–1429. doi:10.1016/j.rser.2016.03.006

Smith, K. R., Khalil, M. A. K., Rasmussen, R. A., Thorneloe, S. A., Manegdeg, F., and Apte, M. (1993). Greenhouse Gases from Biomass and Fossil Fuel Stoves in Developing Countries: a Manila Pilot Study. *Chemosphere* 26, 479–505. doi:10.1016/0045-6535(93)90440-g

Stine, W. B., and Diver, R. B. (1994). *A Compendium of Solar Dish/Stirling Technology*. Albuquerque, NM (United States): Sandia National Labs.

Sup, B. A., Zainudin, M. F., Ali, T. Z. S., Bakar, R. A., and Ming, G. L. (2015). Effect of Rim Angle to the Flux Distribution Diameter in Solar Parabolic Dish Collector. *Energ. Proced.* 68, 45–52. doi:10.1016/j.egypro.2015.03.231

Tucker, M. (1999). Can Solar Cooking Save the Forests? *Ecol. Econ.* 31, 77–89. doi:10.1016/s0921-8009(99)00038-5

Wentzel, M., and Pouris, A. (2007). The Development Impact of Solar Cookers: a Review of Solar Cooking Impact Research in South Africa. *Energy policy* 35, 1909–1919. doi:10.1016/j.enpol.2006.06.002

Yadav, V., Kumar, Y., Agrawal, H., and Yadav, A. (2017). Thermal Performance Evaluation of Solar Cooker with Latent and Sensible Heat Storage Unit for Evening Cooking. *Aust. J. Mech. Eng.* 15, 93–102. doi:10.1080/14484846.2015.1093260

Yahuza, I., Rufai, Y., and Tanimu, L. (2016). Design, Construction and Testing of Parabolic Solar Oven. *J. Appl. Mech. Eng.* 5.

Yettou, F., Gama, A., Azoui, B., Malek, A., and Panwar, N. L. (2019). Experimental Investigation and thermal Modelling of Box and Parabolic Type Solar Cookers for Temperature Mapping. *J. Therm. Anal. Calorim.* 136, 1347–1364. doi:10.1007/s10973-018-7811-9

Zamani, H., Moghiman, M., and Kianifar, A. (2015). Optimization of the Parabolic Mirror Position in a Solar Cooker Using the Response Surface Method (RSM). *Renew. Energ.* 81, 753–759. doi:10.1016/j.renene.2015.03.064

NOMENCLATURE

A Area (m^2)

C Concentration ratio

D Diameter (mm)

f focal length (mm)

$h_{c,i-gls}$ convective heat transfer coefficient from air to glass (W/m^2 K)

$h_{c,gls-a}$ convective heat transfer coefficient from glass to ambient (W/m^2 K)

$h_{c,p-i}$ convective heat transfer coefficient from cooking pot to enclosed air (W/m^2 K)

$h_{c,v-i}$ convective heat transfer coefficient from the cooking vessel to enclosed air (W/m^2 K)

$h_{r,gls-s}$ radiative heat transfer coefficient from glass to the pot surface (W/m^2 K)

$h_{r,pot-gls}$ radiative heat transfer coefficient from cooking pot to glass (W/m^2 K)

$h_{r,v-gls}$ radiative heat transfer coefficient from the cooking vessel to glass (W/m^2 K)

$h_{c,ref-a}$ radiative heat transfer coefficient from the reflector to ambient (W/m^2 K)

$h_{c,pot-a}$ convective heat transfer coefficient from the cooking pot to ambient (W/m^2 K)

$h_{c,pot-wat}$ convective heat transfer coefficient from the cooking pot to water (W/m^2 K)

$h_{r,pot-ref}$ radiative heat transfer coefficient from air to glass (W/m^2 K)

$h_{r,pot-s}$ radiative heat transfer coefficient from the pot to the cover surface (W/m^2 K)

$h_{c,ref-s}$ convective heat transfer coefficient from the reflector to the pot surface (W/m^2 K)

$h_{r,ref-s}$ radiative heat transfer coefficient from the reflector to the pot surface (W/m^2 K)